



RESEARCH PAPER

The specialised pro-resolving lipid mediator maresin 1 reduces inflammatory pain with a long-lasting analgesic effect

Victor Fattori¹  | Felipe A. Pinho-Ribeiro¹ | Larissa Staurengo-Ferrari¹ | Sergio M. Borghi¹ | Ana C. Rossaneis¹ | Rubia Casagrande² | Waldiceu A. Verri Jr.¹ 

¹Department of Pathology, Centre of Biological Sciences, Londrina State University, Londrina, Brazil

²Department of Pharmaceutical Sciences, Centre of Health Science, Londrina State University, Londrina, Brazil

Correspondence

Waldiceu A. Verri Jr, Departamento de Ciências Patológicas, Universidade Estadual de Londrina, Rodovia Celso Garcia Cid KM480 PR445, PO Box 10.011, Londrina, Paraná 86057-970, Brazil.
Email: waverri@uel.br; waldiceujr@yahoo.com.br

Funding information

Central Multiusuário de Laboratórios de Pesquisa from Londrina State University (CMLP-UEL); Conselho Nacional de Desenvolvimento Científico e Tecnológico; Coordination for the Improvement of Higher Education Personnel (CAPES, Brazil); Department of Science and Technology from the Science, Technology and Strategic Inputs Secretariat of the Ministry of Health (Decit/SCTIE/MS, Brazil) intermediated by National Council for Scientific and Technological Development (CNPq, Brazil) with support of Araucária Foundation and State Health Secretariat, Paraná (SESA-PR, Brazil); Funding Authority for Studies and Projects and State Secretariat of Science, Technology and Higher Education (MCTI/FINEP/CT-INFRA-PROINFRA, Brazil), Grant/Award Number: 01.12.0294.00 and 01.13.0049.00; Programa de Apoio a Grupos de Excelência (PRONEX) grant supported by SETI/Araucária Foundation and MCTI/CNPq, and Paraná State Government, Grant/Award Number: agreement 014/2017, protocol 46.843; Central Multiusuário de Laboratórios de Pesquisa; Paraná State Government, Grant/Award Number: 014/2017; MCTI/CNPq; SETI/Araucária Foundation; Funding Authority for Studies and Projects and State Secretariat of Science, Technology and Higher Education, Grant/Award Number: 01.13.0049.00 01.12.0294.00; Department of Science and Technology, Grant/Award Number: 041/2017

Background and Purpose: Maresin 1 (MaR1) is a specialised pro-resolving lipid mediator with anti-inflammatory and analgesic activities. In this study, we addressed the modulation of peripheral and spinal cord cells by MaR1 in the context of inflammatory pain.

Experimental Approach: Mice were treated with MaR1 before intraplantar injection of carrageenan or complete Freund's adjuvant (CFA). Mechanical hyperalgesia was assessed using the electronic von Frey and thermal hyperalgesia using a hot plate. Spinal cytokine production and NF- κ B activation were determined by ELISA and astrocytes and microglia activation by RT-qPCR and immunofluorescence. CGRP release by dorsal root ganglia (DRG) neurons was determined by EIA. Neutrophil and macrophage recruitment were determined by immunofluorescence, flow cytometry, and colorimetric methods. *Trpv1* and *Nav1.8* expression and calcium imaging of DRG neurons were determined by RT-qPCR and Fluo-4AM respectively.

Key Results: MaR1 reduced carrageenan- and CFA-induced mechanical and thermal hyperalgesia and neutrophil and macrophage recruitment proximal to CGRP⁺ fibres in the paw skin. Moreover, MaR1 reduced NF- κ B activation, IL-1 β and TNF- α production, and spinal cord glial cells activation. In the DRG, MaR1 reduced CFA-induced *Nav1.8* and *Trpv1* mRNA expression and calcium influx and capsaicin-induced release of CGRP by DRG neurons.

Conclusions and Implications: MaR1 reduced DRG neurons activation and CGRP release explaining, at least in part, its analgesic and anti-inflammatory effects. The enduring analgesic and anti-inflammatory effects and also post-treatment activity of MaR1 suggest that specialised pro-resolving lipid mediators have potential as a new class of drugs for the treatment of inflammatory pain.

Abbreviations: ALX/FRP2, N-formyl peptide receptor 2; CFA, complete Freund's adjuvant; DRG, dorsal root ganglia; IBA-1, ionised calcium-binding adapter molecule 1; MaR1, maresin 1 (IUPAC: 7R,14S-dihydroxy-4Z,8E,10E,12Z,16Z,19Z-docosahexaenoic acid); MPO, myeloperoxidase; NAG, N-acetyl- β -D-glucosaminidase; Rv, resolvin; SPMs, specialised pro-resolving lipid mediators; TRPV1, transient receptor potential cation channel subfamily V member 1

1 | INTRODUCTION

Nociceptive pain is essential for the maintenance of bodily integrity. Inflammatory pain, on the other hand, induces mechanical and thermal hypersensitivity, which occur in the absence of noxious stimuli. Therefore, it represents an important type of pain given that it can be pathological if not properly managed. In fact, when inadequately managed, the perception of acute pain can be worsened due to impairment in sleep (Alexandre et al., 2017; Sinatra, 2010). An exacerbation of pain occurs due to the sensitisation of specialised sensory neurons, namely, nociceptors, leading to a state known as hyperalgesia (Verri et al., 2006). In the periphery sensitisation is mediated by several inflammatory mediators, such as **PGE₂**, **histamine**, and cytokines, released by immune cells such as mast cells, neutrophils, and macrophages (Fattori, Hohmann, et al., 2017; Pinho-Ribeiro, Verri, & Chiu, 2017). In the spinal cord, this sensitisation is mediated by cytokines, chemokines, and growth factors released by glial cells, namely, microglia, astrocytes, and oligodendrocytes (Fattori, Borghi, et al., 2017; Scholz & Woolf, 2007; Zarpelon et al., 2016).

Over the past decade, the mechanism thought to be responsible for the resolution of the acute inflammatory process has changed. Compelling evidence has demonstrated that the resolution of inflammation is an active process (Chiang & Serhan, 2017; Serhan, 2017; Serhan, Chiang, Dalli, & Levy, 2015). Once thought to be a passive process, it is now known to be tightly regulated by omega-3 fatty acid-derived molecules, so-called specialised pro-resolving lipid mediators (SPMs; Serhan, 2017). With regards to pain, SPMs, namely, resolvin (Rv) **RvE1**, RvE2, RvE3, RvD1, RvD2, and maresin 1 (MaR1), were identified in human synovial fluids of patients with arthritis (Giera et al., 2012). The presence of these mediators was negatively associated with pain score, indicating that they possibly control pain (Giera et al., 2012). Isolated SPMs have been successively used as therapeutic drugs in different models, including pain models (Chiang & Serhan, 2017). They possess efficacy at very low doses, usually in the ng to µg range (Serhan et al., 2015). For instance, intrathecal treatment with RvE1 at 10 ng reduces inflammatory pain via spinal and peripheral mechanisms by acting on **chemerin receptor 1 (also known as Chem23)**, which is expressed by dorsal root ganglia (DRG) neurons and in the spinal cord (Xu et al., 2010). Of interest, RvE1 reduced the second phase of formalin-induced overt pain-like behaviour in a dose 1,000 times lower than morphine, indicating a potent analgesic effect (Xu et al., 2010). Their clinical relevance was demonstrated in a meta-analysis study showing that supplementation with omega-3 fatty acids for 3 to 4 months reduces patient-reported joint pain intensity, minutes of morning stiffness, and consumption of nonsteroidal anti-inflammatory drugs (Goldberg & Katz, 2007). SPMs act on GPCRs, which can be either selective for an SPM or shared with other SPMs (Chiang & Serhan, 2017; Chiurchiu et al., 2016; J. Gu et al., 2018; Park, 2015; Serhan et al., 2015; Xu et al., 2010; Zhang et al., 2017). Evidence suggests that MaR1 shares the **ALX/FP2** receptor with D-series Rv and lipoxins (J. Gu et al., 2018; Zhang et al., 2017). However, ligand-binding

What is already known

- Maresin 1 (MaR1) reduces neuropathic pain and capsaicin-induced pain-like behaviour.
- MaR1 reduces microglia and astrocyte activation.

What this study adds

- MaR1 reduces inflammatory pain with a long-lasting analgesic effect.
- MaR1 reduces capsaicin-induced activation and CGRP release by dorsal root ganglia neurons and leukocyte counts near CGRP+ fibres.

What is the clinical significance

- MaR1 is effective at low doses and is active as a pre- or post-treatment.
- The long-lasting analgesic effect of MaR1 might be useful for the treatment of chronic pain.

assays are required to further confirm this interaction and whether the effect of MaR1 depends solely on agonism of ALX/FP2. In trigeminal ganglion and DRG neurons, the inhibitory effects of MaR1 on **capsaicin**-induced transient receptor potential cation channel subfamily V member 1 (**TRPV1**) currents were blocked after treatment with pertussis toxin, suggesting that it can act on a Gai-coupled GPCR pathway (Park, 2015; Serhan et al., 2012). MaR1 is a **docosahexaenoic acid** (DHA)-derived SPM produced by macrophages and possesses potent anti-inflammatory activity, which is related mainly to the inhibition of neutrophil recruitment and stimulation of efferocytosis by macrophages (Francos-Quijorna et al., 2017; Serhan et al., 2012; Serhan et al., 2015). Furthermore, in a model of spinal cord injury, the endogenous production of MaR1 begins only 14 days after injury, and exogenous administration of it at early time points induces spinal cord recovery, indicating neuroprotective and pro-resolving effects (Francos-Quijorna et al., 2017). MaR1 also demonstrates analgesic activity in different models of pain (Gao et al., 2018; Park, 2015; Serhan et al., 2012; Zhang et al., 2018). Treatment with MaR1 reduces capsaicin-induced overt pain-like behaviour, vincristine-induced neuropathic pain (Serhan et al., 2012), complete Freund's adjuvant (CFA)-induced temporomandibular pain (Park, 2015), spinal nerve ligation-induced neuropathic pain (Gao et al., 2018), and tibial bone fracture-induced pain (Zhang et al., 2018). However, to date, there is no study addressing the modulation of DRG neurons and immune cells (in the periphery and spinal cord) by MaR1 in the context of peripheral inflammatory pain. For that reason, we studied the effect of MaR1, administered intrathecally, on carrageenan- and CFA-induced pain, which are two well-established experimental models for the screening of new drugs for pain relief.

2 | METHODS

2.1 | Animals

All experiments were performed in accordance with the International Association for Study of Pain guidelines and with the approval of the Londrina State University Ethics Committee on Animal Research and Welfare (process numbers 4014.2015.70 and 12766.2015.54). In this study, we used healthy male Swiss and LysM-eGFP mice (8 weeks of age, 25 ± 1 g [RRID:MGJ:2654932]) from Londrina State University, Paraná, Brazil. Mice were randomly assigned and housed in standard clear plastic cages, kept in light/dark cycle of 12:12 hr with ad libitum water and food. Behavioural testing was performed between 9 a.m. and 5 p.m. in a room maintained at a temperature of $21^\circ\text{C} \pm 1^\circ\text{C}$. A block randomisation method was used to randomise subjects into groups resulting in equal sample sizes at all time points. The investigators were blinded to the treatments. All efforts were made to minimise the number of animals used and their suffering. Animal studies are reported in compliance with the ARRIVE guidelines (Kilkenny et al., 2010) and with the recommendations made by the *British Journal of Pharmacology*. Animals were killed by the application of isoflurane as an anaesthetic (5% in oxygen using a precision vaporiser) followed by decapitation as a confirmation method. A total of 588 Swiss mice and 72 LysM-eGFP were used in this study. No animals were excluded from statistical analysis.

2.2 | Experimental procedures

Mice were treated once with 1, 3, or 10 ng of MaR1 (Cayman Chemical, Ann Arbor, MI, USA) or vehicle (10% ethanol) via an i.t. route (between L4 and L6 spinal segments, 10 μl) and under isoflurane anaesthesia (3% in oxygen using a precision vaporiser), 20 min before intraplantar injection of carrageenan (100 $\mu\text{g}/20 \mu\text{l}$ per paw) or CFA (10 μl per paw). The stock solution contained 1 $\text{ng}\cdot\mu\text{l}^{-1}$ of MaR1 in 100% ethanol and was kept in a -80°C freezer. Caution was taken to avoid exposure of MaR1 to air during the preparation for treatment. Findings from a previous study indicate that i.t. delivery of 10% ethanol produces a mild and transient analgesic effect, which is observed 30 min after delivery but not after 1 hr (Xu et al., 2010). Based on that study, all behavioural experiments involving pretreatment with MaR1 were performed 1 hr after the stimulus (1:20 hr after MaR1 treatment). The exceptions were those experiments involving pretreatment with MaR1 on the CFA-induced pain model, which were conducted 1 day after treatment. Mechanical and thermal hyperalgesia were evaluated 1–5 hr after carrageenan injection or for 7 days after CFA injection. The optimum dose of MaR1 (10 ng) was chosen for the following experiments based on mechanical and thermal hyperalgesia. The spinal cord was dissected 3 hr after carrageenan injection to determine cytokine production (TNF- α and IL-1 β) and NF- κB activation by ELISA. Hind paw skin was dissected 5 hr after carrageenan injection to determine neutrophil and macrophage recruitment by immunofluorescence, flow cytometry, and enzymatic assays. In the other set of experiments,

the spinal cord was dissected 3 days after CFA injection to determine cytokine production (TNF- α and IL-1 β) and NF- κB activation by ELISA. To determine activation of glial cells, the spinal cord was dissected 3 days after CFA injection. Hind paw skin was dissected 3 days after CFA injection to determine neutrophil and macrophage recruitment by immunofluorescence, flow cytometry, and enzymatic assays. Ipsilateral DRGs (from L4 to L6 spinal cord segments) were also dissected 3 days after CFA injection to determine *Trpv1* and *Nav1.8* mRNA expression by RT-qPCR and calcium imaging using confocal microscopy. For CFA-induced overt pain-like behaviour (flinches and time spent licking the paw), mice were treated once with 10 ng of MaR1 or vehicle (10% ethanol) i.t. 1 day before intraplantar injection of CFA (10 μl per paw). To assess the efficacy of the post-treatment with MaR1, mice received MaR1 at 10 ng or vehicle (10% ethanol), i.t., 1 or 3 days after being stimulated with with CFA. In this set of experiments, all behavioural assays were performed 1:20 hr post-treatment. CGRP release was determined using DRG neuron cultures. Cells were treated with MaR1 (0.3, 1, or 3 $\text{ng}\cdot\text{ml}^{-1}$) before addition of the stimulus, capsaicin (500 nM, 1 hr).

2.3 | Mechanical hyperalgesia

Mechanical hyperalgesia was evaluated by the electronic version of von Frey's filaments, as reported previously (Cunha et al., 2004). In a quiet, temperature-controlled room, mice were gently placed in acrylic cages (12 \times 10 \times 17 cm) with wire grid floors, 30 min before the start of testing. The test consisted of evoking a hind paw flexion reflex with a handheld force transducer (electronic aesthesiometer, Insight, Ribeirão Preto, SP, Brazil) adapted with a 0.5-mm² polypropylene tip. The investigator was trained to apply the tip perpendicularly to the central area of the plantar hind paw with a gradual increase in pressure. The upper limit of pressure was 15 g. The endpoint was characterised by the removal of the member followed by clear paw flinching or paw licking movements. After paw withdrawal, the intensity of the pressure was automatically recorded, with the final response value being obtained from the average of three measurements. The animals were tested before and after treatments. The results are expressed as delta (Δ) withdrawal threshold (in g), which was calculated by subtracting the mean measurements at 1–5 hr after carrageenan injection or 1–7 days after CFA injection, from the zero-time (baseline values) mean measurements. The investigators were blinded to the treatment.

2.4 | Thermal hyperalgesia

Heat thermal hyperalgesia was performed using a hot plate at $55^\circ\text{C} \pm 1^\circ\text{C}$ (Insight, Ribeirão Preto, SP, Brazil), as previously described (Calixto-Campos et al., 2015). The reaction time was registered when one of the following responses (endpoints) were observed: clear paw flinching, paw licking, or jumping. The results were calculated by subtracting the values obtained 1–5 hr after carrageenan injection or 1–7 days after CFA injection, from the zero-time (baseline values)

measurement. The results are expressed as delta (Δ) withdrawal latency (in s). A cut-off of 20 s was set to avoid tissue damage (Fattori et al., 2015). The investigators were blinded to the treatment.

2.5 | Cytokine measurement

For cytokine production, the spinal cord was homogenised into 500 μ l of PBS buffer containing protease inhibitors. TNF- α and IL-1 β levels were determined by ELISA using eBioscience kits (eBioscience, San Diego, CA, USA) according to the manufacturer's instructions. Reading was performed at 450 nm (Multiskan GO Microplate Spectrophotometer, Thermo Scientific, Vantaa, Finland). The results are expressed as pg of each cytokine \cdot mg⁻¹ of protein.

2.6 | NF- κ B activation

Spinal cord was dissected into ice-cold lysis buffer (Cell Signaling Technology, Beverly, MA, USA). The homogenates were centrifuged (16,100 g, 10 min, 4°C), and the supernatants were used to assess the levels of total and phosphorylated NF- κ B p65 subunit by ELISA using PathScan kits #7836 and #7834, respectively (Cell Signaling Technology) according to the manufacturer's instructions. The results are presented as the sample OD ratio (sample OD from total p65 subunit divided by sample OD phosphorylated p65 subunit) measured at 450 nm (Multiskan GO Microplate Spectrophotometer, Thermo Scientific).

2.7 | MPO and NAG activities

Neutrophil [myeloperoxidase (MPO) activity] and macrophage [N-acetyl- β -D-glucosaminidase (NAG) activity] recruitment were evaluated using a colorimetric assay as described previously (Ruiz-Miyazawa et al., 2015). Samples of the hind paw skin were dissected into ice-cold 50-mM K₂HPO₄ buffer (pH 6.0) containing 0.5% hexadecyltrimethylammonium bromide and kept at -80°C until use. Samples were homogenised and centrifuged at 16,100 g, 2 min, 4°C. For MPO activity, 10 μ l of the supernatant was mixed with 200 μ l of 50-mM phosphate buffer, pH 6.0, containing 0.167-mg \cdot ml⁻¹ o-dianisidine dihydrochloride and 0.015% hydrogen peroxide. Reading was performed after 15 min at 450 nm (Multiskan GO Microplate Spectrophotometer, Thermo Scientific). The results are presented as MPO activity (number of neutrophils \times 10⁴ \cdot mg⁻¹ of protein). For NAG activity, 20 μ l of supernatant was obtained as described for the MPO activity assay and added to a 96-well plate. The reaction was initiated by adding 2.24 mM of 4-nitrophenyl N-acetyl- β -D-glucosaminide. Then the plate was incubated at 37°C for 10 min, and the reaction was stopped by the addition of 100 μ l of 0.2-M glycine buffer, pH 10.6. Reading was performed at 405 nm (Multiskan GO Microplate Spectrophotometer, Thermo Scientific). The results are presented as NAG activity (macrophages \times 10⁴ \cdot mg⁻¹ of protein).

2.8 | Overt pain-like behaviour

The total number of paw flinches and time spent licking the paw were counted during the 30 min after injection CFA as previously described (Calixto-Campos et al., 2015). Results are expressed as the total number of flinches or time spent licking the paw (in s) performed in 30 min. The investigators were blinded to the treatment.

2.9 | RT-qPCR

DRG or spinal cord were dissected into TRIzol™ reagent, and total RNA was isolated according to manufacturer's instructions. The purity of total RNA was measured with a spectrophotometer, and the wavelength absorption ratio (260/280 nm) was between 1.8 and 2.0 for all preparations. Reverse transcription of total RNA to cDNA and qPCR were performed using GoTaq® 2-Step RT-qPCR System (Promega, Madison, WI, USA) on a StepOnePlus™ Real-Time PCR System (Applied Biosystems®, Thermo Fisher Scientific, Waltham, MA, USA). The relative gene expression was determined using the comparative 2^{- $\Delta\Delta$ Ct} method. The primers sequence used in this study were *Trpv1* sense: 5'-TTCCTGCAGAAGAGCAAGAAGC-3', *Trpv1* antisense: 5'-CCCATTGTGCAGATTGAGCAT-3'; *Nav1.8* sense: 5'-GTGTGCATGACCCGAAGTAT-3', *Nav1.8* antisense: 5'-CAAAACCTCTTGCCAGTATCT-3'; *Gfap* sense: 5'-GGCGCTCAATGCTGGCTTCA-3', antisense: 5'-TCTGCCTCCAGCCTCAGGTT-3'; *Iba-1* sense: 5'-ATGGAGTTTGATCTGAATGGAAT-3', antisense: 5'-TCAGGGCAGCTCGGAGATAGCTTT-3'; and *β -actin* sense: 5'-AGCTGCGTTTTACACCCTTT-3', *β -actin* antisense: 5'-AAGCCATGCCAATGTTGTCT-3'. The expression of *β -actin* mRNA was used as a reference gene to normalise data.

2.10 | Immunofluorescence staining

Spinal cord segments from regions L4-L6 were dissected and post-fixed, and then were replaced overnight with 30% sucrose. Spinal cord segments were embedded in optimum cutting temperature, and 15 or 40 μ m (only for CGRP⁺ fibres staining) sections were cut in a cryostat and processed for immunofluorescence. For microglia staining, sections were blocked and then incubated with primary antibodies anti-ionised calcium-binding adapter molecule 1 (IBA-1; 1:400, cat #PA5-27436, Thermo Fisher Scientific; RRID:AB_2544912). After that, sections for IBA-1 were stained with secondary antibody Alexa Fluor 488 (1:1,000, cat #A-11008, Thermo Fisher Scientific; RRID:AB_143165). For astrocyte staining, we used an anti-gial fibrillary acidic protein antibody conjugated with Alexa Fluor 488 (1:1,000, cat #MAB3402X, MilliporeSigma, Burlington, MA, USA; RRID:AB11210273). In the hind paw skin, neutrophils were stained using anti-Ly-6G/Ly-6C (Gr-1) antibody conjugated with Alexa Fluor 488 (1:200, clone RB6-8C5, BioLegend, San Diego, CA, USA; RRID:AB_313366). Macrophages were stained using anti-CD68 (1:500, cat #ab125212, Abcam, Cambridge, MA, USA; RRID:AB10975465) followed by the secondary antibody DyLight 594 (1:200, cat #DI-1594, Peterborough, UK; RRID:AB_2336413).

CGRP⁺ fibres were stained with anti-CGRP (1:500, cat #C8198, MilliporeSigma; RRID:AB_259091) followed by the secondary antibody Alexa Fluor 647 (1:500, cat# ab150075, Abcam; RRID:AB_2752244), and leukocytes were stained with anti-CD11b (1:250, clone 5C6, cat #MCA711, Bio-Rad, Hercules, CA, USA; RRID:AB_321292) followed by the secondary antibody Alexa Fluor 594 (1:500, Jackson ImmunoResearch Laboratories, West Grove, PA, USA; RRID:AB_2340689). The images and analysis were performed using a Confocal Microscope (TCS SP8, Leica Microsystems, Mannheim, Germany).

The immuno-related procedures used comply with the recommendations made by the *British Journal of Pharmacology*.

2.11 | Flow cytometry

Hind paw skin was dissected, minced, and then incubated for 2 hr (37°C, while shaking) in 2 ml of HEPES-buffered saline (MilliporeSigma) containing collagenase P, as described previously (Pinho-Ribeiro et al., 2018). After this incubation, cells were gently dissociated and filtered through a 40- μ m mesh and mixed washing buffer consisting of HBSS (Thermo Fisher Scientific) and 0.5% BSA. Cells were centrifuged for 5 min at 300 g, supernatant was discarded, and the pellet was resuspended in 500 μ l of washing buffer. The cell suspension was incubated on ice with mouse FcR Blocking Reagent (Miltenyi Biotec, Cambridge, MA, USA) for 10 min and then incubated for 30 min on ice with the following antibodies (BioLegend): Zombie Aqua™ Fixable Viability Kit (1:1,000), anti-CD45-PE (1:200, clone 30-F11; RRID:AB_2563597), anti-CD11b-Brilliant Violet 605™ (1:200, clone M1/70; RRID:AB_11126744), anti-F4/80-APC (1:200, clone BM8; RRID:AB_893493), and anti-Ly6G-FITC (1:200, clone 1A8; RRID:AB_968318). Cells were centrifuged for 5 min at 300 g, and the pellet was resuspended in 500 μ l of washing buffer 2% PFA. FACS data were analysed and plotted using FlowJo software (FlowJo LLC; RRID:SCR_008520).

2.12 | Calcium imaging

Calcium imaging of DRG neurons was performed as previously described (Chiu et al., 2013). DRGs were dissected into Neurobasal-A medium (Life Technologies, Thermo Fisher Scientific), dissociated in collagenase A (1 mg·ml⁻¹)/dispase II (2.4 U·ml⁻¹; RocheApplied Sciences, Indianapolis, IN, USA) in HEPES-buffered saline (MilliporeSigma) for 70 min at 37°C. After trituration with glass Pasteur pipettes of decreasing size, DRG cells were centrifuged over a 10% BSA gradient, plated on laminin-coated cell culture dishes. DRGs were then loaded with 1.2 μ M of Fluo-4AM in Neurobasal-A medium, incubated for 30 min 37°C, washed with HBSS, and imaged in a Confocal Microscope (TCS SP8, Leica Microsystems). To assess TRPV1 activation, DRG plates were recorded for 6 min, which was divided in 2 min of initial reading (0-s mark, baseline values), following by stimulation with capsaicin for 2 min at the 120-s mark (1 μ M, TRPV1 agonist; Fattori, Hohmann, Rossaneis, Pinho-Ribeiro, & Verri,

2016) and KCl for 2 min at the 240-s mark (40 mM, activates all neurons). Calcium flux was analysed from the mean fluorescence measured with the LAS X Software (Leica Microsystems).

2.13 | CGRP release

DRG neurons (5,000 per well) were cultured for 1 week in Neurobasal-A medium (Life Technologies, Thermo Fisher Scientific) with half of the medium being replaced with fresh media every 2 days as described previously (Pinho-Ribeiro et al., 2018). Neurons received vehicle or different concentrations of MaR1 (0.3–3 ng·ml⁻¹) before stimulus with capsaicin (500 nM) for 1 hr at 37°C, 5% of CO₂. Supernatant was collected to determine CGRP concentration using a CGRP EIA kit according to the manufacturer's instructions (Cayman Chemical).

2.14 | Data and statistical analysis

Results are presented as means \pm SEM of measurements made on six mice in each group per experiment. Each experiment was conducted twice. Data were analysed using the software GraphPad Prism version 6.01 (La Jolla, CA, USA [RRID:SCR_002798]). Two-way repeated measure ANOVA, followed by Tukey's post hoc, was used to analyse data from experiments of multiple time points (mechanical and thermal hyperalgesia). With data from experiments of a single time point, one-way ANOVA was used followed by Tukey's post hoc test. Statistical differences were considered significant when $P < 0.05$. The data and statistical analysis comply with the recommendations of the *British Journal of Pharmacology* on experimental design and analysis in pharmacology.

2.15 | Nomenclature of targets and ligands

Key protein targets and ligands in this article are hyperlinked to corresponding entries in <http://www.guidetopharmacology.org>, the common portal for data from the IUPHAR/BPS Guide to PHARMACOLOGY (Harding et al., 2018), and are permanently archived in the Concise Guide to PHARMACOLOGY 2017/18 (Alexander, Christopoulos, et al., 2017; Alexander, Fabbro, et al., 2017; Alexander, Striessnig, et al., 2017).

3 | RESULTS

3.1 | MaR1 reduces carrageenan-induced hyperalgesia and neutrophil and macrophage recruitment

First, we evaluated the efficacy of intrathecal treatment with MaR1 in carrageenan-induced mechanical and thermal hyperalgesia. Treatment with 10 ng of MaR1 reduced carrageenan-induced mechanical (Figure 1a) and thermal (Figure 1b) hyperalgesia. To determine leukocyte recruitment, it used LysM-eGFP mice (Figure 2a) and staining for GR-1 (neutrophil marker, Figure 2b) or CD68

FIGURE 1 MaR1 reduces carrageenan-induced mechanical and thermal hyperalgesia. Mechanical hyperalgesia (a) and thermal hyperalgesia (b) were evaluated 1, 3, and 5 hr after intraplantar injection of carrageenan (100 μg per paw). Results from mechanical hyperalgesia are presented as Δ withdrawal threshold (in g) and for thermal hyperalgesia as Δ withdrawal threshold (in s), which was calculated by subtracting the mean measurements at 1–5 hr after carrageenan from the zero-time (baseline values) mean measurements. MaR1 reduced carrageenan-induced mechanical (a) and thermal (b) hyperalgesia. Results are representative of two independent experiments and are presented as mean \pm SEM of measurements, $n = 6$ mice per group per experiment ($*P < 0.05$ vs. saline, $\#P < 0.05$ vs. 0 $\text{mg}\cdot\text{kg}^{-1}$ group; two-way repeated measures ANOVA followed by Tukey's post-test)

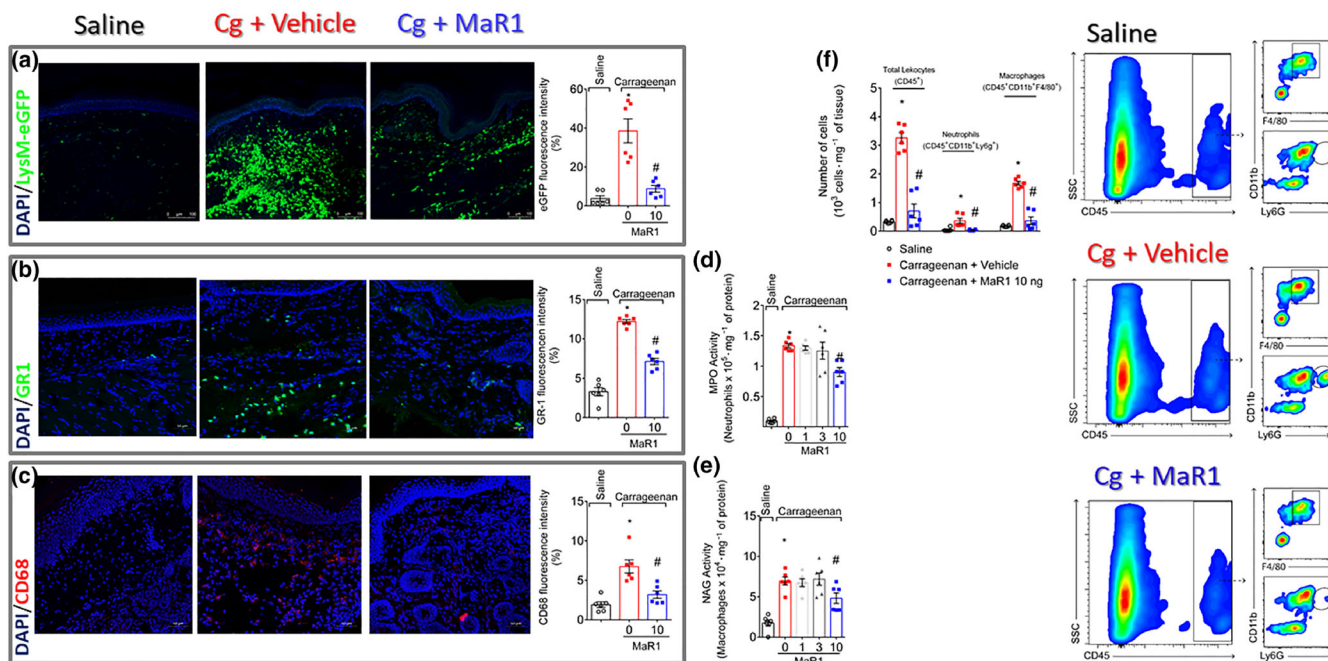
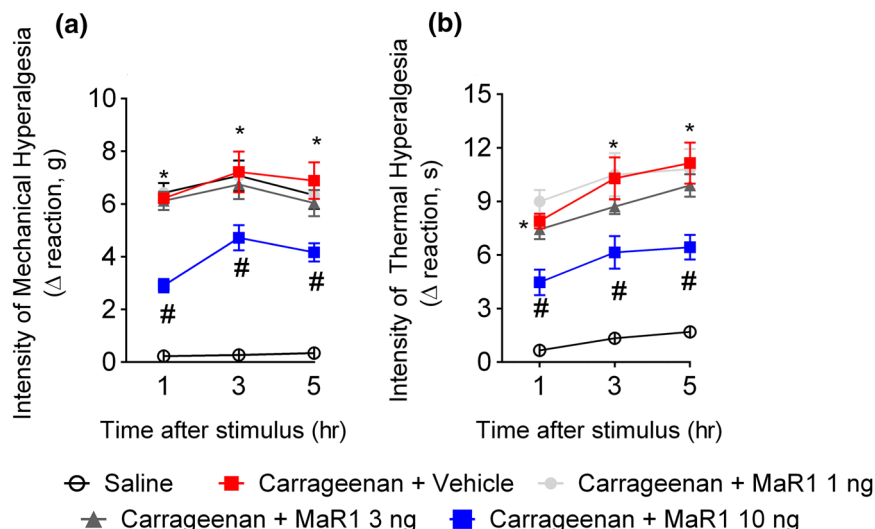


FIGURE 2 MaR1 inhibits carrageenan-induced neutrophil and macrophage recruitment to the hind paw skin. Hind paw skin of LysM-eGFP (neutrophil and macrophage marker, a) or Swiss (b–f) mice was dissected for determination of neutrophil (GR-1 staining [b], MPO activity [d], and flow cytometry [CD11b⁺Ly6G⁺ cells, f]) and macrophage (CD68 staining [c], NAG activity [e], and flow cytometry [CD11b⁺F4/80⁺ cells, f]) recruitment 5 hr after carrageenan stimulus. LysM-eGFP mouse, immunofluorescence, enzymatic activity, and flow cytometry data show that MaR1 reduced carrageenan-induced recruitment of neutrophils and macrophages in the paw skin. Results are expressed as mean \pm SEM, $n = 6$ mice per group per experiment, two independent experiments ($*P < 0.05$ vs. saline, $\#P < 0.05$ vs. 0 $\text{mg}\cdot\text{kg}^{-1}$ group; one-way ANOVA followed by Tukey's post-test)

(macrophage marker, Figure 2c). We observed a reduction in carrageenan-induced neutrophil and macrophage recruitment to the hind paw as observed by the reduced intensity of fluorescence of these cellular markers and their respective enzymatic activity (MPO and NAG, respectively; Figure 2d,e). For the quantification of these

cells, flow cytometry was performed. Treatment with MaR1 reduced both CD11b⁺Ly6G⁺ neutrophils and CD11b⁺F4/80⁺ macrophages recruitment to the paw skin (Figure 2f). Therefore, this dose was chosen for the following experiments involving the intraplantar injection of carrageenan.

3.2 | MaR1 inhibits carrageenan-induced spinal cord cytokine production and NF- κ B activation

The efficacy of MaR1 in carrageenan-induced spinal cord cytokine production and NF- κ B activation were then investigated. Carrageenan increased spinal cord TNF- α (Figure 3a) and IL-1 β (Figure 3b) production and NF- κ B (Figure 3c) activation as observed by the reduction in total-p65/phosphorylated-p65 OD ratio. The ratio was obtained by dividing the OD measured from total-p65 by the OD measured from phosphorylated-p65. Therefore, a decrease in the ratio is attributed to higher levels of phosphorylated p65 subunit (Ser536 residue), which indicates the activation of the NF- κ B signalling pathway. Importantly, these parameters were reduced after intrathecal treatment with MaR1 (Figure 3).

3.3 | MaR1 reduces CFA-induced mechanical and thermal hyperalgesia

Next, we sought to evaluate the efficacy of MaR1 in a chronic model of pain. For that, it used intraplantar stimulus with CFA. A single treatment with 10 ng of MaR1 reduced mechanical (Figure 4a) and thermal (Figure 4b) hyperalgesia, which lasted for 5 days after the stimulus. Both doses of 1 and 3 ng reduced mechanical and thermal hyperalgesia starting 2 days after CFA injection and lasting until the fifth day after the stimulus. The effect of MaR1 at 10 ng initiated at Day 1 after the stimulus; therefore, this dose was chosen for the following experiments involving the intraplantar injection of CFA. To assess the efficacy of MaR1 in already established pain, mice received intrathecal treatment with MaR1 at 10 ng or vehicle, 1 (Figure 4c,d) or 3 days (Figure 4e,f) after stimulus with CFA. A single treatment with MaR1 1 day after the stimulus displayed analgesic effect that lasted for 3 days (Figure 4c,d). Treatment with this SPM 3 days after the stimulus showed a less potent analgesic effect, which lasted for 2 days (Figure 4e,f). These set of data show that a single intrathecal

administration of MaR1 presents a long-lasting analgesic effect as a pretreatment and post-treatment.

3.4 | MaR1 decreases CFA-induced overt pain-like behaviour

Spontaneous pain is a common symptom of patients with chronic pain (Fattori, Borghi, et al., 2017). CFA not only induce chronic pain but also overt pain-like behaviour (Calixto-Campos et al., 2015). Thus, the efficacy of MaR1 in CFA-induced overt pain-like behaviour was then evaluated. Mice were treated once with 10 ng of MaR1 (intrathecal) or vehicle (10% ethanol, intrathecal) 1 day before intraplantar injection of CFA (10 μ l per paw). This time point was chosen considering that only the dose of MaR1 at 10 ng reduced CFA-induced hyperalgesia at Day 1 after the stimulus (Figure 4a,b). Treatment with MaR1 at 10 ng reduced CFA-induced flinches (Figure 5a) and time spent licking the paw (Figure 5b).

3.5 | MaR1 inhibits neutrophil and macrophage recruitment close to CGRP⁺ fibres in the hind paw skin and the release of CGRP by DRG neurons

Once activated, neurons release **neuropeptides**, such as CGRP, to modulate the recruitment and activation of immune cells during inflammation (Pinho-Ribeiro et al., 2017). In the inflammatory site, recruited neutrophils and macrophages have an important role in the genesis and maintenance of pain. Thus, we next addressed whether treatment with MaR1 could reduce the recruitment of these cells to the hind paw skin. In the first set of data, we wonder whether there would be leukocytes close to CGRP⁺ fibres. We observed a lower number of leukocytes (CD11b⁺ cells) close to CGRP⁺ fibres in the CFA + MaR1 group than the CFA + vehicle group (Figure 6a). Given that we observed a lower number of leukocytes close to CGRP⁺ fibres and a reduction in neuronal activation, we next investigated the influence of this SPM on the release of CGRP by DRG neurons. Previous

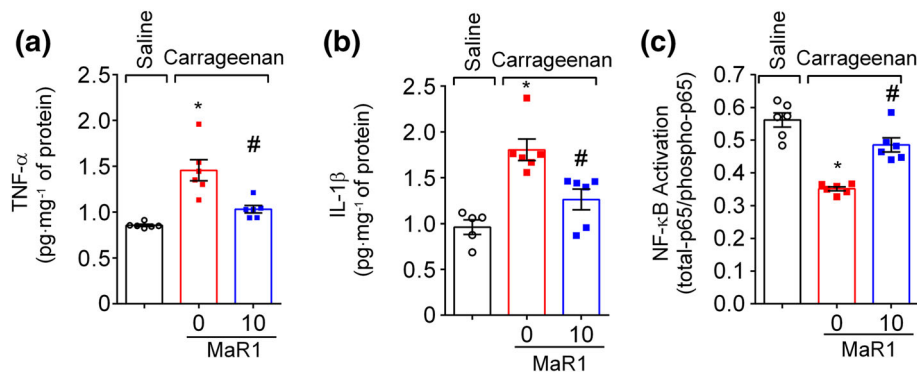


FIGURE 3 MaR1 inhibits carrageenan-induced spinal cord cytokine production and NF- κ B activation. Three hours after intraplantar injection of carrageenan (100 μ g per paw), the spinal cord was dissected for determination of TNF- α (a), IL-1 β (b), and NF- κ B activation (c) by ELISA. NF- κ B activation was observed as a reduction of total p65/phosphorylated p65 OD ratio. Results are representative of two independent experiments and are presented as mean \pm SEM, $n = 6$ mice per group per experiment (* $P < 0.05$ vs. saline, # $P < 0.05$ vs. 0 mg·kg⁻¹ group; one-way ANOVA followed by Tukey's post-test)

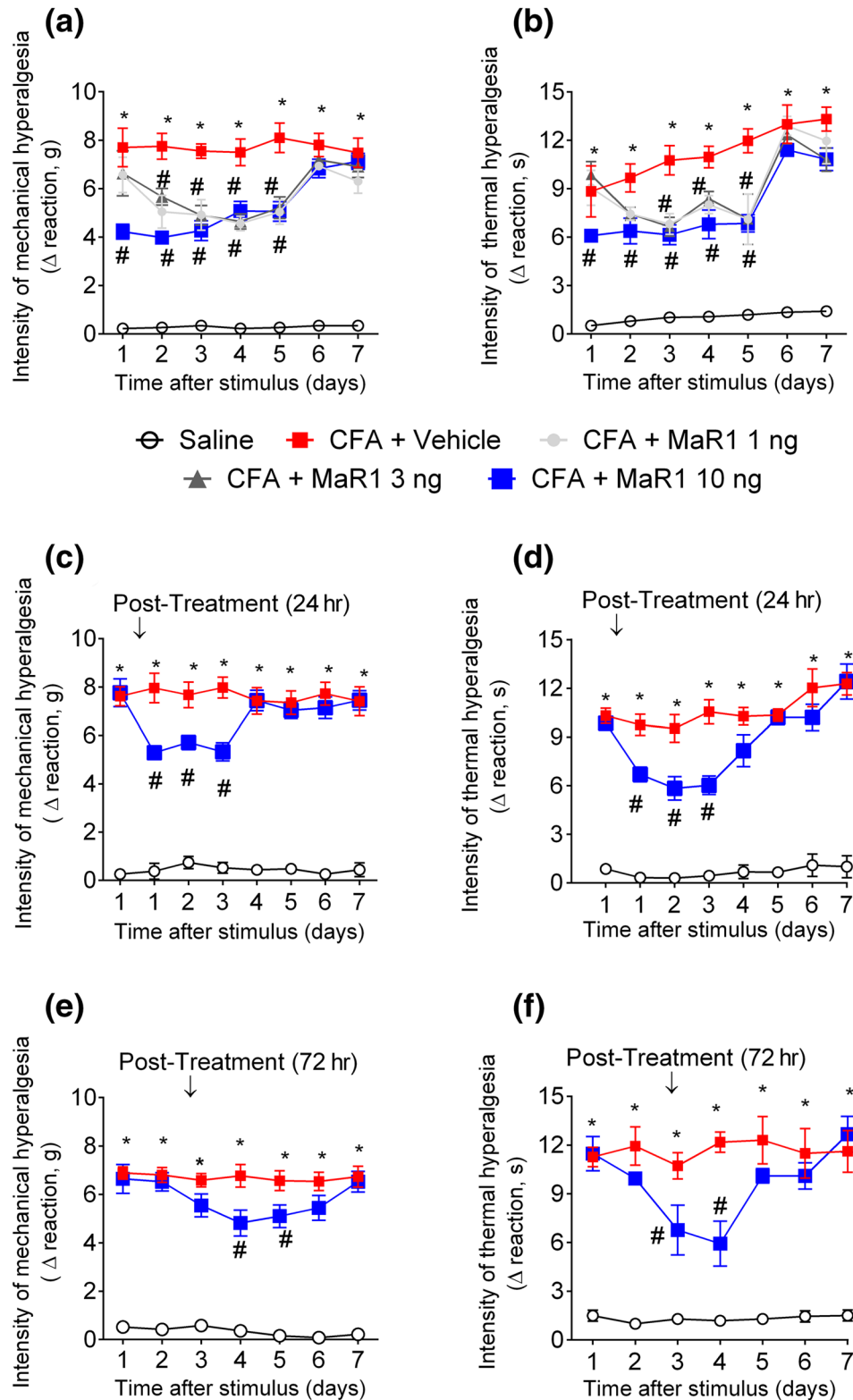


FIGURE 4 MaR1 reduces CFA-induced mechanical and thermal hyperalgesia. Mechanical hyperalgesia (a, c, and e) and thermal hyperalgesia (b, d, and f) were evaluated 1–7 days after intraplantar injection of CFA (10 μ l per paw). Results from mechanical hyperalgesia are presented as Δ withdrawal threshold (in g) and for thermal hyperalgesia as Δ withdrawal threshold (in s), which were calculated by subtracting the mean measurements at 1–7 days after carrageenan from the zero-time (baseline values) mean measurements. Panels (a) and (b) show the analgesic effect of MaR1 as a 20 min pretreatment. Panels (c) and (d) show the analgesic effect of MaR1 as a post-treatment 1 day after CFA. The measurements on the first day (c and d) were shown before and after treatment. Panels (e) and (f) show the analgesic effect of MaR1 as a post-treatment 3 days after CFA. Results are representative of two independent experiments and are presented as mean \pm SEM of measurements, $n = 6$ mice per group per experiment (* $P < 0.05$ vs. saline, # $P < 0.05$ vs. 0 mg·kg⁻¹ group; two-way repeated measures ANOVA followed by Tukey's post-test)

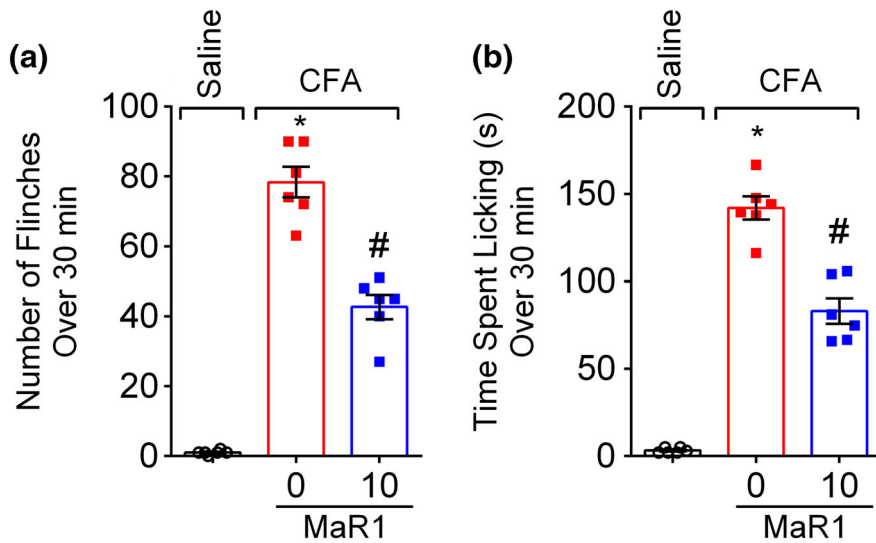


FIGURE 5 MaR1 decreases CFA-induced overt pain-like behaviour. CFA induced repetitive paw flinches (a) and licking of the paw (b), which were determined over 30 min 1 day after intraplantar injection of CFA (10 μ l per paw). Results are representative of two independent experiments and are presented as mean \pm SEM, $n = 6$ mice per group per experiments (* $P < 0.05$ vs. saline, # $P < 0.05$ vs. 0 mg·kg⁻¹ group; one-way ANOVA followed by Tukey's post-test)

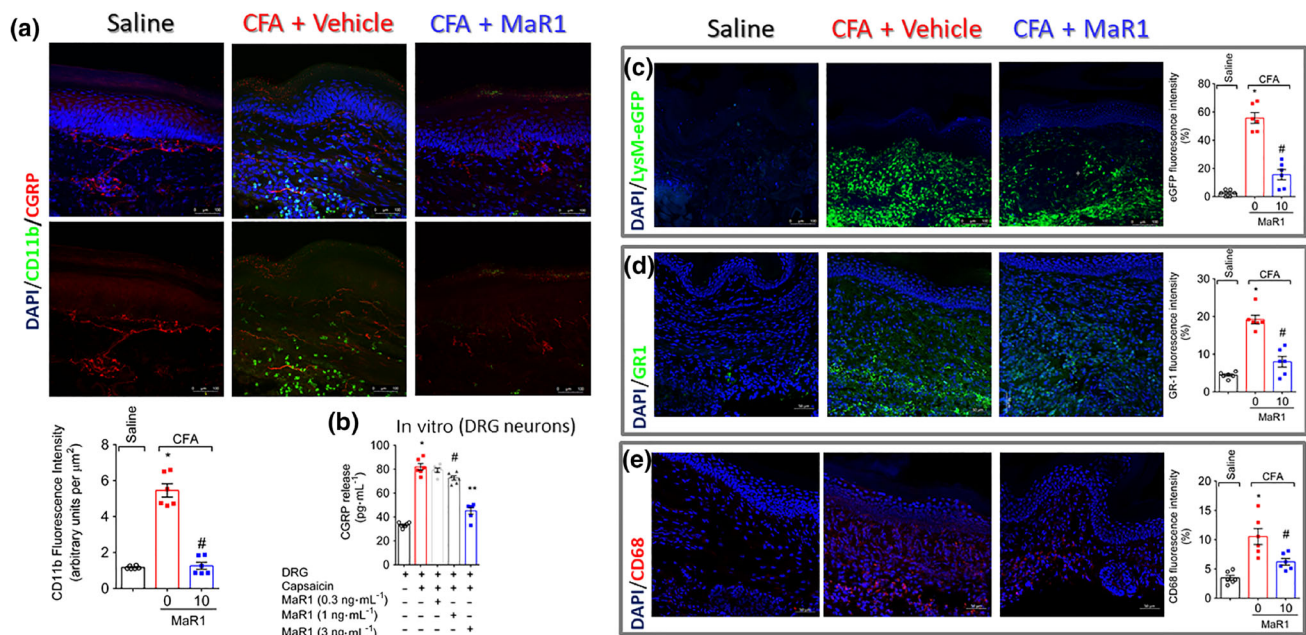


FIGURE 6 MaR1 reduces the number of leukocytes proximal to CGRP⁺ fibres and the release of CGRP by DRG neurons. Hind paw skin was dissected for determination of total leukocytes (CD11b⁺ cells) close to CGRP⁺ fibres (a), which showed an increase of total CD11b fluorescence proximal to CGRP⁺ fibres in the CFA group and reduction after MaR1 treatment. For CGRP release assay (b), naïve DRG neurons received vehicle or different concentrations of MaR1 (0.3, 1, or 3 ng·mL⁻¹) before stimulus with capsaicin. Supernatant was collected 1 hr after capsaicin to determine CGRP levels by EIA. Panels (c) to (e) analysed with further detail the cellular types recruited to the paw skin during CFA inflammation. LysM-eGFP (C57BL/6 background mice) was used to determine neutrophils and macrophages (c). The staining neutrophils (GR-1, d) and macrophages (CD68, e) in hind paw skin samples of Swiss mice also showed that MaR1 reduced CFA-induced recruitment of these cells. Results are expressed as mean \pm SEM, $n = 6$ mice per group per experiment, two independent experiments (* $P < 0.05$ vs. saline, # $P < 0.05$ vs. 0 mg·kg⁻¹ group; one-way ANOVA followed by Tukey's post-test). Results are expressed as mean \pm SEM, $n = 6$ wells per group per experiment, two independent experiments (* $P < 0.05$ vs. saline, # $P < 0.05$ vs. vehicle group; ** $P < 0.05$ vs. 1 ng·mL⁻¹ group; one-way ANOVA followed by Tukey's post-test)

report indicates that MaR1 completely blocks current in TRPV1⁺ DRG neurons as observed by whole cell patch-clamp (Serhan et al., 2012). Herein, we show that MaR1 reduced capsaicin-induced CGRP release in DRG neuron culture in a concentration-dependent manner (Figure 6 b). The concentration of 3 ng·mL⁻¹ of MaR1 was statistically different

when compared to the concentration of 1 ng·mL⁻¹. To further determine which cell types were reduced after treatment with MaR1, it used LysM-eGFP mice (neutrophil and macrophage marker, Figure 6 c) and staining for GR-1 (neutrophil marker, Figure 6d) or CD68 (macrophage marker, Figure 6e). Treatment with MaR1 reduced

CFA-induced neutrophil and macrophage. To have a better quantification and profiling of these cells, flow cytometry was performed. MaR1 reduced the recruitment of both CD11b⁺Ly6G⁺ neutrophils and CD11b⁺F4/80⁺ macrophages (Figure 7a) and their respective enzymatic activities as observed by the MPO and NAG activity assays (Figure 7b,c).

3.6 | MaR1 inhibits CFA-induced spinal cord cytokine production and NF- κ B activation

The next step was to evaluate the efficacy of MaR1 in CFA-induced spinal cord cytokine production and NF- κ B activation. CFA induced TNF- α (Figure 8a) and IL-1 β (Figure 8b) production, which were

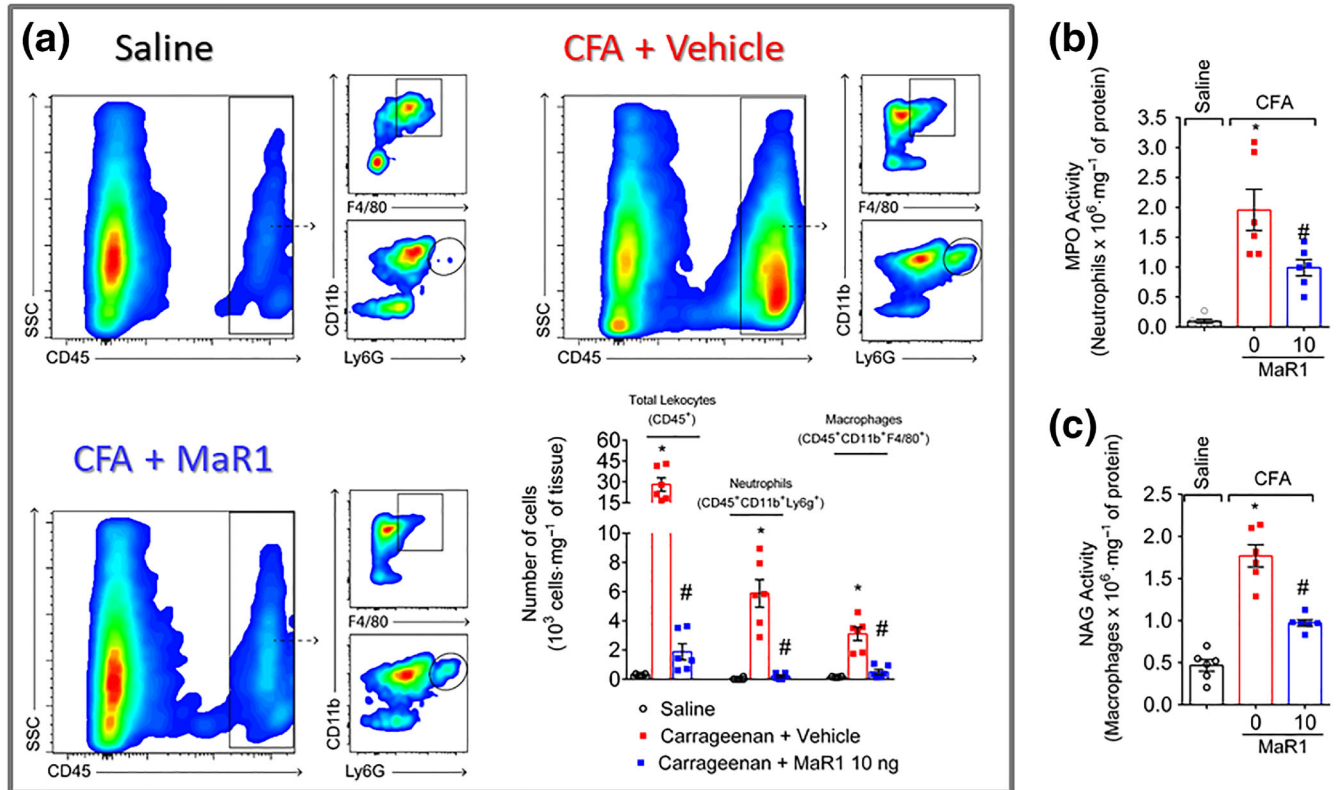


FIGURE 7 MaR1 inhibits CFA-induced CD11b⁺Ly6G⁺ neutrophils and CD11b⁺F4/80⁺ macrophage recruitment to the hind paw skin. Hind paw skin was dissected for determination of neutrophil (flow cytometry [a]) and MPO activity [b]) and macrophage recruitment (flow cytometry [a]) and NAG activity [c]) 3 days after the stimulus. Results are expressed as mean \pm SEM, $n = 6$ mice per group per experiment, two independent experiments ($P < 0.05$ vs. saline, $\#P < 0.05$ vs. 0 mg kg⁻¹ group; one-way ANOVA followed by Tukey's post-test)

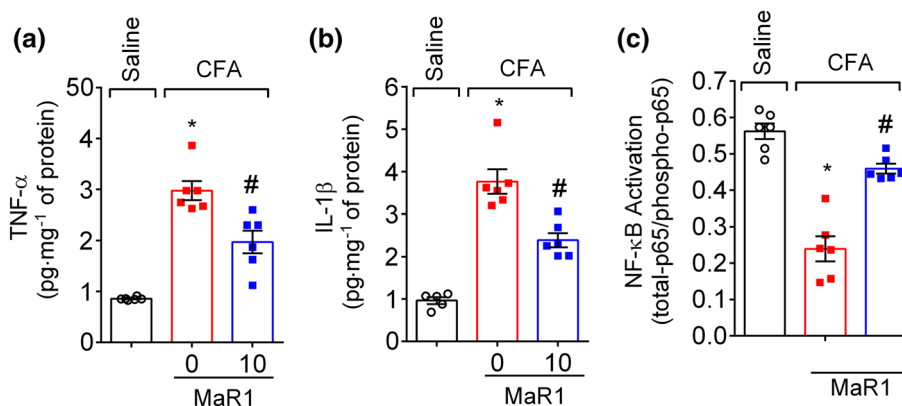


FIGURE 8 MaR1 inhibits CFA-induced spinal cord cytokine production and NF- κ B activation. Three days after intraplantar injection of CFA (10 μ l per paw), the spinal cord was dissected for determination of TNF- α (a), IL-1 β (b), and NF- κ B activation (c) by ELISA. NF- κ B activation was observed as a reduction of total p65/phosphorylated p65 OD ratio. Results are representative of two independent experiments and are presented as mean \pm SEM, $n = 6$ mice per group per experiments ($*P < 0.05$ vs. saline, $\#P < 0.05$ vs. 0 mg kg⁻¹ group; one-way ANOVA followed by Tukey's post-test)

reduced after treatment with MaR1. In addition, CFA induced NF- κ B activation (Figure 8c) as observed by the reduction in total-p65/phosphorylated-p65 OD ratio. The ratio was obtained by dividing the OD measured from total-p65 by the OD measured from phosphorylated-p65. Therefore, a decrease in the ratio is attributed to higher levels of phosphorylated p65 subunit (Ser536 residue) relative to total-p65, which indicates the activation of the NF- κ B signalling pathway. Importantly, a single treatment with 10 ng of MaR1 reduced spinal cord NF- κ B activation and pro-inflammatory cytokine production.

3.7 | MaR1 decreases CFA-induced activation of astrocytes and microglia

Given the role of glial cells in the development of pain (Fattori, Borghi, et al., 2017; Scholz & Woolf, 2007), we next assessed the efficacy of MaR1 in CFA-induced spinal cord activation of astrocytes and microglia. Treatment with MaR1 reduced CFA-induced activation of

astrocytes [glial fibrillary acidic protein (GFAP)—astrocyte activation marker] and microglia (IBA-1—microglia activation marker) as observed by the reduction in both mRNA (Figure 9a,b) and intensity of fluorescence (Figure 9c,d).

3.8 | MaR1 reduces CFA-induced DRG neurons activation

Activation of DRG neurons can be observed through an increase in calcium influx (Blake et al., 2018; Chiu et al., 2013). Thus, we wondered whether DRG neurons from CFA-stimulated mice would present a higher response to capsaicin than DRG neurons from mice that received intraplantar saline and whether there would be modulation of this response by MaR1 treatment. DRG neurons from CFA-stimulated mice presented a higher baseline level of calcium influx than DRG neurons from saline mice (Figure 10a–c). Importantly, MaR1 reduced CFA elevation of baseline calcium levels. As

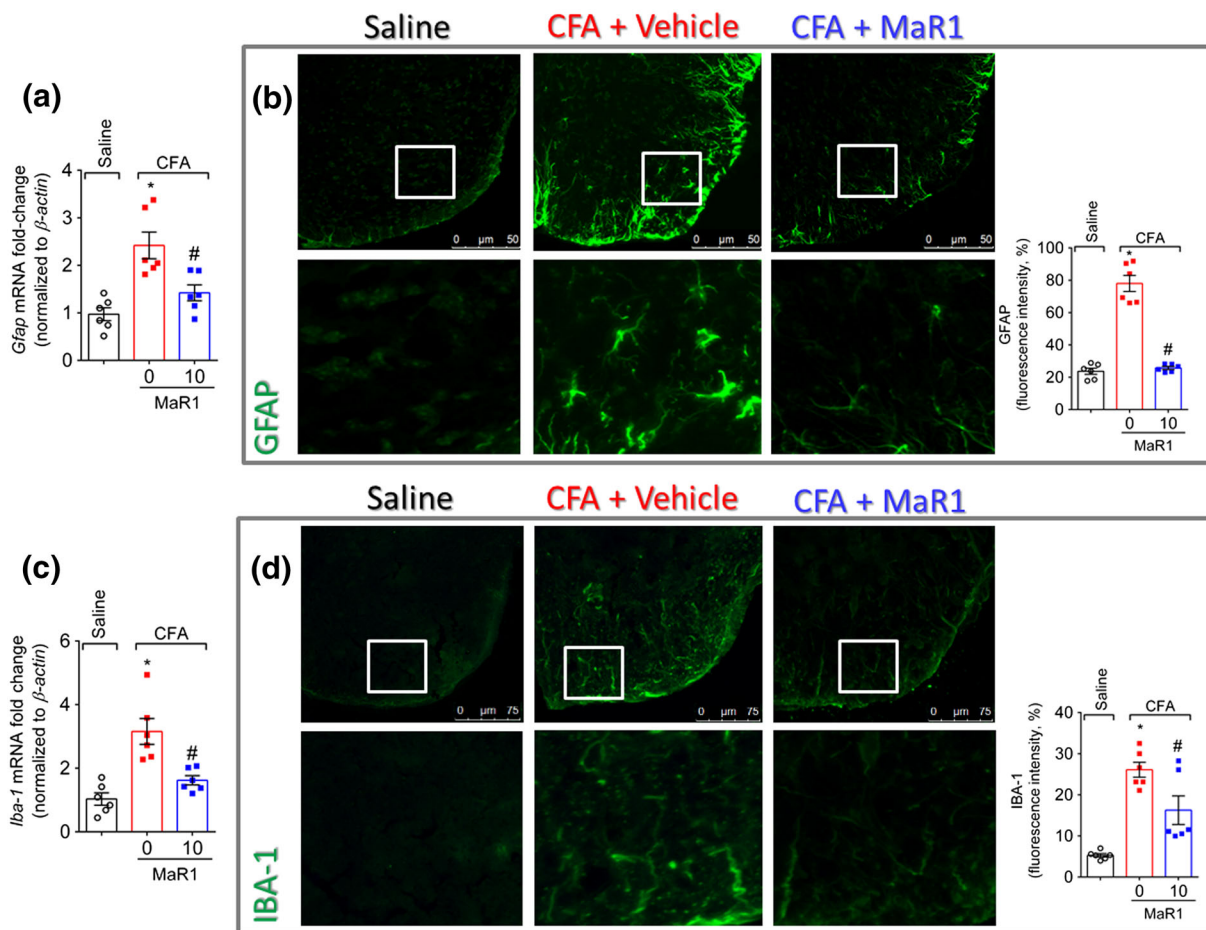


FIGURE 9 MaR1 decreases CFA-induced astrocyte and microglia activation. Three days after intraplantar injection of CFA (10 μ l per paw), spinal cord was dissected for determination of astrocyte and microglia activation by RT-qPCR (a and c) and by immunofluorescence (b and d). Glial fibrillary acidic protein (GFAP) was used as a marker of the activation of astrocytes (a and b), and IBA-1 was used as a marker of microglia activation (c and d). Results are representative of two independent experiments and are presented as mean \pm SEM, $n = 6$ mice per group per experiments (* $P < 0.05$ vs. saline, # $P < 0.05$ vs. 0 mg·kg $^{-1}$ group, ** $P < 0.05$ vs. 10 mg·kg $^{-1}$; one-way ANOVA followed by Tukey's post-test)

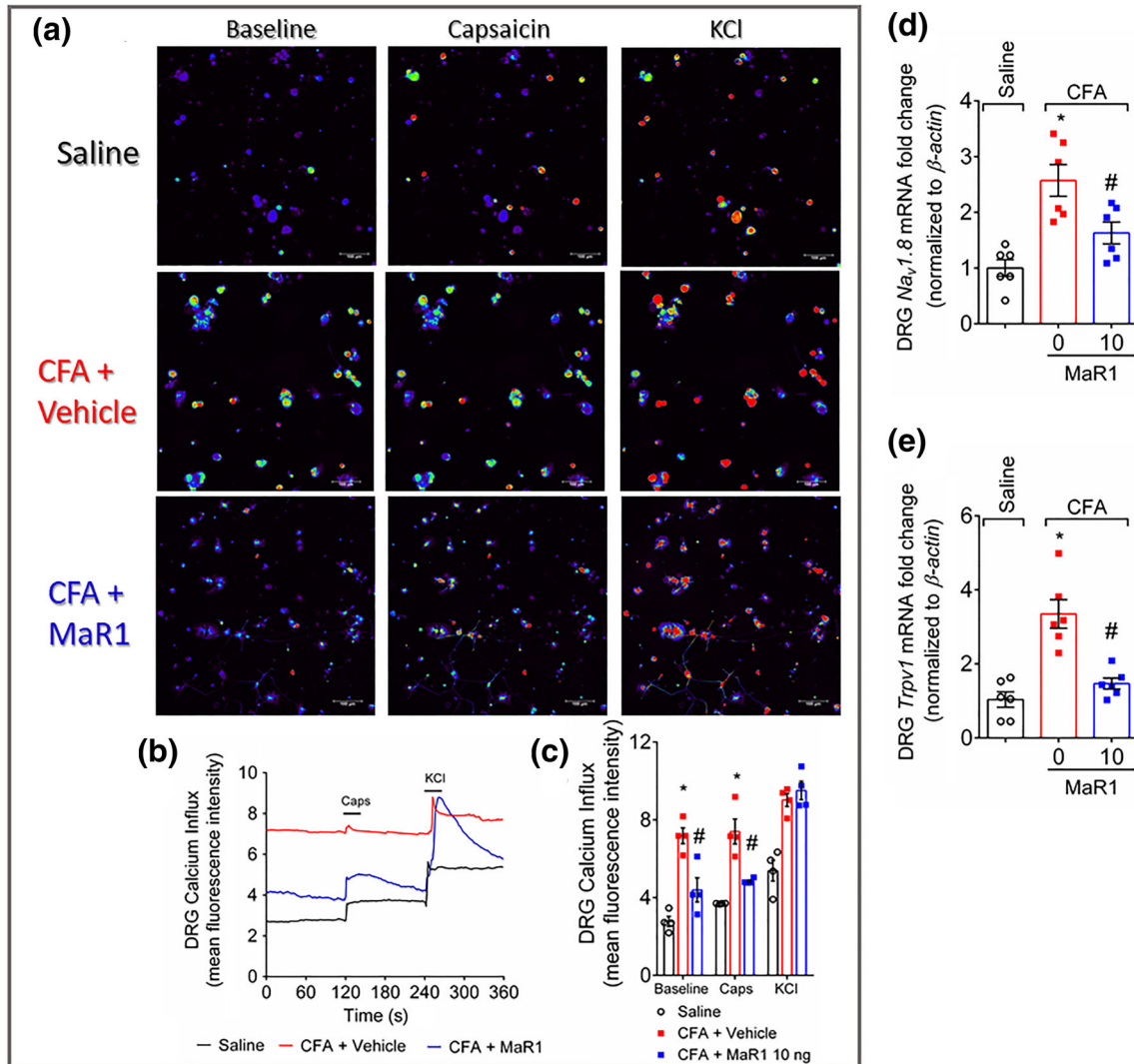


FIGURE 10 MaR1 reduces CFA-induced activation of DRG neurons. Three days after intraplantar injection of CFA (10 μ l per paw), DRGs were dissected for calcium imaging using Fluo-4AM (a–c) and mRNA expression by RT-qPCR (d and e). Panel (a) displays representative fields of DRG neurons dissected from saline-treated mice, mice stimulated with CFA and treated with vehicle, or stimulated with CFA and treated with MaR1. Panel (a): baseline fluorescence (first column), fluorescence after capsaicin (second column), and after KCl control (third column). Panel (b) displays the fluorescence intensity traces of calcium influx from the representative DRG fields (a) throughout the 6 min of recording. The representative traces show that the CFA + vehicle DRG neurons presented higher calcium levels in the baseline than saline control and CFA + MaR1 DRG neurons groups. Panel (c) shows the mean fluorescence intensity of calcium influx of the baseline (0-s mark) and that following the stimulus, either capsaicin (120-s mark, TRPV1 agonist) or KCl (240-s mark, activates all neurons). Panels (d) and (e) show the DRG neurons RT-qPCR data demonstrating that MaR1 reduced CFA-induced *Nav1.8* (d) and *Trpv1* (e) mRNA expression. Results are expressed as mean \pm SEM, $n = 4$ DRG plates (each plate is a neuronal culture pooled from six mice) per group per experiment, and RT-qPCR used $n = 6$ DRG per group per experiment, two independent experiments ($*P < 0.05$ vs. saline, $\#P < 0.05$ vs. 0 mg·kg $^{-1}$ group; one-way ANOVA followed by Tukey's post-test)

an increase on calcium flux is indicative of DRG neuron activation, these data suggest that MaR1 reduces the activation of DRG neurons in CFA-induced inflammation. In line with the reduction of DRG neurons activation by MaR1, treatment with it reduced the CFA-induced mRNA expression of *Nav1.8* (Figure 10d) and *Trpv1* (Figure 10e) in the DRG, which are channels involved in nociceptor sensory neuron sensitisation and activation resulting in pain (Chiu et al., 2014). Therefore, MaR1 reduced CFA-induced DRG neurons activation and the expression of markers of nociceptor sensory neurons sensitisation.

4 | DISCUSSION

The intrathecal treatment with the SPM MaR1 reduces inflammatory pain induced by carrageenan and CFA showing a long-lasting analgesic profile. A single intrathecal pretreatment with MaR1 at 10 ng reduced CFA-induced hyperalgesia for 5 days, while a 24 hr post-treatment reduced CFA-induced hyperalgesia for 3 days. These data indicate that MaR1 presents a potent and long-lasting analgesic effect, which could be useful in the management of pain of inflammatory origin. The analgesic effect of MaR1 is related to the inhibition of

inflammation-induced activation of astrocytes and microglia, reduction in NF- κ B activation, and thereby TNF- α and IL-1 β production. In the periphery, MaR1 reduced the recruitment of leukocytes and the number of leukocytes close to CGRP⁺ fibres. Data also demonstrated the link between intrathecal MaR1 treatment with its peripheral anti-inflammatory and analgesia effects. MaR1 decreased CFA-induced DRG mRNA expression of pain-related channels *Nav1.8* and *Trpv1* and the activation of DRG neurons (as observed by lower baseline levels of calcium influx), which resulted in reduced CGRP release.

The resolution of inflammation relies on temporal changes in the production of lipid mediators (Bannenberg et al., 2005; Levy, Clish, Schmidt, Gronert, & Serhan, 2001). A study analysing approximately 300 miRNAs shows that the shift on lipid mediators production impacts on the expression of miRNAs that are hierarchically clustered at different time points towards resolution (Recchiuti & Serhan, 2012). For instance, RvD1 reduces zymosan-induced inflammation by increasing the miR-21, which regulates IL-10 production at later time points (12 and 24 hr after zymosan when compared to 4 hr; Recchiuti & Serhan, 2012). This indicates that SPMs control specific miRNAs in a time-dependent manner to promote resolution of acute inflammation (Recchiuti & Serhan, 2012). In addition, after stimulus with zymosan, the number of macrophages with a pro-resolving phenotype gradually increases (48 to 72 hr after stimulus), which also correlates with the resolution of inflammation (Bannenberg et al., 2005). These findings are consistent with the fact that some isolated SPMs also present time-dependent efficacy. For instance, a single intrathecal treatment with RvD1 before the development of tactile allodynia produces an enduring analgesic effect that lasts for 10 and 30 days in a model of paw incision-induced pain and in a model of skin/muscle incision and retraction surgery-induced pain, respectively (Huang, Wang, Serhan, & Strichartz, 2011). However, treatment with RvD1 at later time points provides limited analgesia (Huang et al., 2011). A single treatment with RvD2 reduces carrageenan-induced mechanical hyperalgesia for 2 days (Park et al., 2011). Focusing on MaR1, peripheral treatment with this SPM shows increasing efficacy over time (14-day period) in a model of vincristine-induced neuropathic pain in mice (Serhan et al., 2012). Thus, this time-dependent effect of SPMs led us to investigate whether the intrathecal treatment with MaR1 could also display a prolonged analgesic profile. In fact, a single pre-treatment with MaR1 provides an analgesic effect for 5 days, while a post-treatment (1 day after stimulus) produces analgesia for 3 days. Altogether, these data indicate that MaR1 presents a long-lasting analgesic effect. Interestingly, the lower doses used in this study showed analgesic effect starting on Day 2 and lasting until Day 5, further indicating time dependency to the analgesic effect of SPMs.

Peripheral inflammatory pain induces changes in the spinal cord circuit that may lead to central sensitisation (Ma & Woolf, 1996; Pinho-Ribeiro et al., 2017; Woolf, 1994). In fact, the CFA model induces central sensitisation with a stronger activation of astrocyte when compared to microglia (Cao et al., 2014; Liao, Hsieh, Huang, & Lin, 2017; Zhu, Zhao, Wang, Gao, & Zhang, 2014). The phenomenon of central sensitisation has been recognised as the main driver of pathological pain leading to plastic changes in the CNS (Scholz & Woolf,

2007; Woolf, 1983). The interaction between glial cells and nociceptor neurons has been linked to these plastic changes that occur in the spinal cord. In rodents, intrathecal treatment with non-selective (e.g., pentoxifylline) or selective glial cell inhibitors (e.g., minocycline for microglia, and fluorocitrate and α -aminoadipate for astrocytes) reduces inflammatory and chronic pain in different experimental settings (Mika, Wawrzczak-Bargiela, Osikowicz, Makuch, & Przewlocka, 2009; Osikowicz et al., 2009; Pavao-de-Souza et al., 2012; Zarpelon et al., 2016). This suggests that targeting spinal cytokines or glial cells might represent important analgesic approaches for treating chronic pain (Fattori, Borghi, et al., 2017; Fattori, Hohmann, et al., 2017; Yekkiral, Roberson, Bean, & Woolf, 2017). We show that intrathecal treatment with MaR1 reduced CFA-induced astrocyte and microglia activation and decreased the production of TNF- α and IL-1 β and NF- κ B activation. Of interest, MaR1 prevents p65 NF- κ B phosphorylation at Ser536 residue (Z. Gu et al., 2016), which is the same residue targeted by the antibody used in the present work. This is important because both cytokines induce neuronal firing, indicating that nociceptor neurons cells respond to these cytokines (Binshtok et al., 2008; Jin & Gereau, 2006). In the spinal cord, TNF- α and IL-1 β also contribute to spinal cord plasticity and thereby central sensitisation (Kawasaki, Zhang, Cheng, & Ji, 2008). Mechanistically, both cytokines enhance the amplitude of AMPA- and glutamate-induced excitatory currents, while only IL-1 β also reduces GABA- and glycine-induced inhibitory transmission in neurons (Kawasaki et al., 2008). In the periphery, these cytokines also contribute to neutrophil recruitment towards tissue and thereby increasing the inflammatory process and pain (Fattori, Amaral, & Verri, 2016; Kolaczowska & Kubek, 2013). The present data indicate a neuronal effect of MaR1, which would ultimately reduce glial cell activation. However, it remains to be determined if MaR1 acts directly in glial cells.

MaR1 blocks TRPV1 with no effect on TRPA1 (Park, 2015; Serhan et al., 2012). This SPM possesses an IC₅₀ of 0.49 ng·ml⁻¹ and completely blocks capsaicin-induced calcium flux with 3 ng·ml⁻¹ (approximately 8.5 nM) in DRG neurons (Serhan et al., 2012). In trigeminal ganglion neurons, MaR1 blocks capsaicin-induced TRPV1 calcium influx in an even lower concentration (0.35 nM; Park, 2015), indicating that it is a potent TRPV1 inhibitor. Thus, to address the effect of MaR1 over TRPV1 activation in our model, DRG neurons from CFA-stimulated mice treated with vehicle or MaR1 were dissected 3 days after the stimulus for calcium imaging and RT-qPCR. A single treatment with MaR1 at 10 ng prevented TRPV1 activation in the DRG neurons (3 days after CFA), as observed by lower baseline levels of calcium influx. Given that an increase in this parameter is indicative of DRG neuron activation (Blake et al., 2018; Chiu et al., 2013), the lower baseline levels of calcium influx that we found suggest that MaR1 reduces CFA-induced DRG neurons activation. In accordance, previous work shows that MaR1 at 0.35 nM reduces CFA-induced spontaneous EPSCs frequency and amplitude in trigeminal neurons in trigeminal neurons (Park, 2015). Thus, these data from trigeminal neurons indicate that MaR1 might reduce spinal cord plastic changes and inhibits central sensitisation via both presynaptic and postsynaptic mechanisms (Park, 2015). Other SPMs,

such as RvD1, RvD2, and RvE1, also possess similar effect on neuronal firing (Park et al., 2011; Xu et al., 2010). For instance, RvE1 at $1 \text{ ng}\cdot\text{ml}^{-1}$ (approximately 2.85 nM) reduces TNF- α -induced spontaneous EPSCs frequency and decreases TNF- α -induced potentiation of NMDA-induced currents in spinal cord neurons (Xu et al., 2010). We observed that MaR1 reduced CFA-induced mRNA expression of the channels *Nav1.8* and *Trpv1*. Strategies targeting these channels are effective at reducing pain (Liao et al., 2017; Yu, Zhao, Guan, & Chen, 2011). Therefore, in addition to reducing neuronal activation (present data and others; Park, 2015; Serhan et al., 2012), it is likely that MaR1 also controls TRPV1 expression in DRG neurons during inflammation.

Upon noxious stimuli, nociceptor neurons release neuropeptides such as CGRP and **substance P** that control the recruitment of immune cells to the inflammatory foci (Pinho-Ribeiro et al., 2017). In fact, ablating or silencing nociceptor sensory neurons modulate sterile and non-sterile inflammation (Blake et al., 2018; Maruyama et al., 2017; Roberson et al., 2013; Talbot et al., 2015). Herein, we show that MaR1 at $3 \text{ ng}\cdot\text{ml}^{-1}$ reduced the release of CGRP by DRG neurons, indicating a possible mechanism by which this SPM reduces inflammation and pain. Thus, the MaR1 inhibition of activation and CGRP release by nociceptor neurons might have contributed to the decreased recruitment of neutrophils and macrophages observed in this work. In fact, MaR1 also reduced the number of neutrophils and macrophages proximal to CGRP⁺ fibres in the paw skin.

5 | CONCLUSION

We demonstrated that MaR1 displays a long-lasting analgesic effect in the nanogram dose range (10 ng per mouse, intrathecal) in pre- and post-treatment protocols. This analgesic effect is related to the inhibition of astrocyte and microglia activation in the spinal cord. Moreover, MaR1 reduced NF- κ B activation and thereby reduced TNF- α and IL-1 β production in the spinal cord. In the periphery, MaR1 reduced the number of leukocytes proximal to CGRP⁺ fibres, and at the DRG level, it decreased the mRNA expression of nociceptor neuron sensitisation-related channels *Nav1.8* and *Trpv1* and reduced DRG neurons activation and CGRP release. The inhibition of CGRP release by nociceptor neurons explains the peripheral effects of MaR1. Given that SPMs present a safe preclinical profile and efficacy at low doses, they might represent a new family of analgesic drugs useful in the treatment of inflammatory pain of chronic and acute nature.

ACKNOWLEDGEMENTS

This work was supported by grants from the Department of Science and Technology from the Science, Technology and Strategic Inputs Secretariat of the Ministry of Health (Decit/SCTIE/MS, Brazil) intermediated by National Council for Scientific and Technological Development (CNPq, Brazil) with support of Araucária Foundation and State Health Secretariat, Paraná (SESA-PR, Brazil; PPSUS Grant agreement 041/2017, protocol 48.095); Funding Authority for Studies

and Projects and State Secretariat of Science, Technology and Higher Education (MCTI/FINEP/CT-INFRA-PROINFRA, Brazil; Grant agreements 01.12.0294.00 and 01.13.0049.00); Programa de Apoio a Grupos de Excelência (PRONEX) grant supported by SETI/Araucária Foundation and MCTI/CNPq; and Paraná State Government (agreement 014/2017, protocol 46.843). We also thank the support of Central Multiusuário de Laboratórios de Pesquisa from Londrina State University (CMLP-UEL). V.F. and F.A.P.-R. acknowledge PhD scholarship from Coordination for the Improvement of Higher Education Personnel (CAPES, Brazil) and CNPq. L.S.-F., A.C.R., and S.M.B. received CNPq Post-Doc fellowship. We also thank Tiago H. Zaninelli and Stephanie Badaro-Garcia for technical assistance.

CONFLICT OF INTEREST

The authors declare no conflicts of interest.

AUTHOR CONTRIBUTIONS

F.A.P.-R. and L.S.-F. treated the animals and injected the stimuli. V.F., S.M.B., and A.C.R. performed behavioural testing. V.F., L.S.-F., A.C.R., and S.M.B. performed confocal microscopy analysis. V.F., F.A.P.-R., L.S.-F., and A.C.R. performed experiments. V.F. and L.S.-F. performed in vitro experiments. V.F., R.C., and W.A.V.J. analysed and interpreted data set. V.F. and W.A.V.J. delineated the study. R.C. and W.A.V.J. received grants and provided essential reagents. V.F. wrote the first draft. V.F. and W.A.V.J. revised and edited the manuscript. All authors read and approved the final version of the manuscript.

DECLARATION OF TRANSPARENCY AND SCIENTIFIC RIGOUR

This Declaration acknowledges that this paper adheres to the principles for transparent reporting and scientific rigour of preclinical research as stated in the *BJP* guidelines for **Design & Analysis**, **Immunoblotting and Immunochemistry**, and **Animal Experimentation**, and as recommended by funding agencies, publishers, and other organisations engaged with supporting research.

ORCID

Victor Fattori  <https://orcid.org/0000-0002-4565-7706>

Waldiceu A. Verri Jr.  <https://orcid.org/0000-0003-2756-9283>

REFERENCES

- Alexander, S. P., Christopoulos, A., Davenport, A. P., Kelly, E., Marrion, N. V., Peters, J. A., ... CGTP Collaborators. (2017). The Concise Guide to PHARMACOLOGY 2017/18: G protein-coupled receptors. *British Journal of Pharmacology*, 174(Suppl 1), S17–S129. <https://doi.org/10.1111/bph.13878>
- Alexander, S. P. H., Fabbro, D., Kelly, E., Marrion, N. V., Peters, J. A., Faccenda, E., ... CGTP Collaborators. (2017). The Concise Guide to PHARMACOLOGY 2017/18: Enzymes. *British Journal of Pharmacology*, 174(S1), S272–S359. <https://doi.org/10.1111/bph.13877>
- Alexander, S. P., Striessnig, J., Kelly, E., Marrion, N. V., Peters, J. A., Faccenda, E., ... CGTP Collaborators. (2017). The Concise Guide to PHARMACOLOGY 2017/18: Voltage-gated ion channels. *British*

- Journal of Pharmacology*, 174(Suppl 1), S160–S194. <https://doi.org/10.1111/bph.13884>
- Alexandre, C., Latremoliere, A., Ferreira, A., Miracca, G., Yamamoto, M., Scammell, T. E., & Woolf, C. J. (2017). Decreased alertness due to sleep loss increases pain sensitivity in mice. *Nature Medicine*, 23(6), 768–774. <https://doi.org/10.1038/nm.4329>
- Bannenberg, G. L., Chiang, N., Ariel, A., Arita, M., Tjonahen, E., Gotlinger, K. H., ... Serhan, C. N. (2005). Molecular circuits of resolution: Formation and actions of resolvins and protectins. *Journal of Immunology*, 174(7), 4345–4355. <https://doi.org/10.4049/jimmunol.174.7.4345>
- Binshtok, A. M., Wang, H., Zimmermann, K., Amaya, F., Vardeh, D., Shi, L., ... Samad, T. A. (2008). Nociceptors are interleukin-1 β sensors. *The Journal of Neuroscience*, 28(52), 14062–14073. <https://doi.org/10.1523/JNEUROSCI.3795-08.2008>
- Blake, K. J., Baral, P., Voisin, T., Lubkin, A., Pinho-Ribeiro, F. A., Adams, K. L., ... Chiu, I. M. (2018). Staphylococcus aureus produces pain through pore-forming toxins and neuronal TRPV1 that is silenced by QX-314. *Nature Communications*, 9(1), 37. <https://doi.org/10.1038/s41467-017-02448-6>
- Calixto-Campos, C., Carvalho, T. T., Hohmann, M. S., Pinho-Ribeiro, F. A., Fattori, V., Manchope, M. F., ... Verri, W. A. Jr. (2015). Vanillic acid inhibits inflammatory pain by inhibiting neutrophil recruitment, oxidative stress, cytokine production, and NF κ B activation in mice. *Journal of Natural Products*, 78(8), 1799–1808. <https://doi.org/10.1021/acs.jnatprod.5b00246>
- Cao, D. L., Zhang, Z. J., Xie, R. G., Jiang, B. C., Ji, R. R., & Gao, Y. J. (2014). Chemokine CXCL1 enhances inflammatory pain and increases NMDA receptor activity and COX-2 expression in spinal cord neurons via activation of CXCR2. *Experimental Neurology*, 261, 328–336. <https://doi.org/10.1016/j.expneurol.2014.05.014>
- Chiang, N., & Serhan, C. N. (2017). Structural elucidation and physiologic functions of specialized pro-resolving mediators and their receptors. *Molecular Aspects of Medicine*, 58, 114–129. <https://doi.org/10.1016/j.mam.2017.03.005>
- Chiu, I. M., Barrett, L. B., Williams, E. K., Strohlich, D. E., Lee, S., Weyer, A. D., ... Woolf, C. J. (2014). Transcriptional profiling at whole population and single cell levels reveals somatosensory neuron molecular diversity. *eLife*, 3. <https://doi.org/10.7554/eLife.04660>
- Chiu, I. M., Heesters, B. A., Ghasemlou, N., Von Hehn, C. A., Zhao, F., Tran, J., ... Woolf, C. J. (2013). Bacteria activate sensory neurons that modulate pain and inflammation. *Nature*, 501(7465), 52–57. <https://doi.org/10.1038/nature12479>
- Chiurchiu, V., Leuti, A., Dalli, J., Jacobsson, A., Battistini, L., Maccarrone, M., & Serhan, C. N. (2016). Proresolving lipid mediators resolvins D1, resolvins D2, and maresin 1 are critical in modulating T cell responses. *Science Translational Medicine*, 8(353), 353ra111.
- Cunha, T. M., Verri, W. A. Jr., Vivancos, G. G., Moreira, I. F., Reis, S., Parada, C. A., ... Ferreira, S. H. (2004). An electronic pressure-meter nociception paw test for mice. *Brazilian Journal of Medical and Biological Research*, 37(3), 401–407. <https://doi.org/10.1590/S0100-879X2004000300018>
- Fattori, V., Amaral, F. A., & Verri, W. A. Jr. (2016). Neutrophils and arthritis: Role in disease and pharmacological perspectives. *Pharmacological Research*, 112, 84–98. <https://doi.org/10.1016/j.phrs.2016.01.027>
- Fattori, V., Borghi, S. M., Rossaneis, A. C., Bertozzi, M. M., Cunha, T. M., & Verri, W. A. Jr. (2017). Neuroimmune regulation of pain and inflammation: Targeting glial cells and nociceptor sensory neurons interaction. In Attar-Rahman, & M. I. Choudhary (Eds.), *Frontiers in CNS drug discovery* (Vol. 3) (pp. 146–200). Sharjah, United Arab Emirates: Bentham Science.
- Fattori, V., Hohmann, M. S., Rossaneis, A. C., Pinho-Ribeiro, F. A., & Verri, W. A. (2016). Capsaicin: Current understanding of its mechanisms and therapy of pain and other pre-clinical and clinical uses. *Molecules*, 21(7). <https://doi.org/10.3390/molecules21070844>
- Fattori, V., Hohmann, M. S. N., Rossaneis, A. C., Manchope, M. F., Alves-Filho, J. C., Cunha, T. M., ... Verri, W. A. Jr. (2017). Targeting IL-33/ST2 signaling: Regulation of immune function and analgesia. *Expert Opinion on Therapeutic Targets*, 21(12), 1141–1152. <https://doi.org/10.1080/14728222.2017.1398734>
- Fattori, V., Pinho-Ribeiro, F. A., Borghi, S. M., Alves-Filho, J. C., Cunha, T. M., Cunha, F. Q., ... Verri, W. A. (2015). Curcumin inhibits superoxide anion-induced pain-like behavior and leukocyte recruitment by increasing Nrf2 expression and reducing NF- κ B activation. *Inflammation Research*, 64(12), 993–1003. <https://doi.org/10.1007/s00011-015-0885-y>
- Francos-Quijorna, I., Santos-Nogueira, E., Gronert, K., Sullivan, A. B., Kopp, M. A., Brommer, B., ... López-Vales, R. (2017). Maresin 1 promotes inflammatory resolution, neuroprotection, and functional neurological recovery after spinal cord injury. *The Journal of Neuroscience*, 37(48), 11731–11743. <https://doi.org/10.1523/JNEUROSCI.1395-17.2017>
- Gao, J., Tang, C., Tai, L. W., Ouyang, Y., Li, N., Hu, Z., & Chen, X. (2018). Pro-resolving mediator maresin 1 ameliorates pain hypersensitivity in a rat spinal nerve ligation model of neuropathic pain. *Journal of Pain Research*, 11, 1511–1519. <https://doi.org/10.2147/JPR.S160779>
- Giera, M., Ioan-Facsinay, A., Toes, R., Gao, F., Dalli, J., Deelder, A. M., ... Mayboroda, O. A. (2012). Lipid and lipid mediator profiling of human synovial fluid in rheumatoid arthritis patients by means of LC-MS/MS. *Biochimica et Biophysica Acta*, 1821(11), 1415–1424. <https://doi.org/10.1016/j.bbali.2012.07.011>
- Goldberg, R. J., & Katz, J. (2007). A meta-analysis of the analgesic effects of omega-3 polyunsaturated fatty acid supplementation for inflammatory joint pain. *Pain*, 129(1–2), 210–223. <https://doi.org/10.1016/j.pain.2007.01.020>
- Gu, J., Luo, L., Wang, Q., Yan, S., Lin, J., Li, D., ... Jin, S. W. (2018). Maresin 1 attenuates mitochondrial dysfunction through the ALX/cAMP/ROS pathway in the cecal ligation and puncture mouse model and sepsis patients. *Laboratory Investigation*, 98, 715–733. <https://doi.org/10.1038/s41374-018-0031-x>
- Gu, Z., Lamont, G. J., Lamont, R. J., Uriarte, S. M., Wang, H., & Scott, D. A. (2016). Resolvin D1, resolvin D2 and maresin 1 activate the GSK3 β anti-inflammatory axis in TLR4-engaged human monocytes. *Innate Immunity*, 22(3), 186–195. <https://doi.org/10.1177/1753425916628618>
- Harding, S. D., Sharman, J. L., Faccenda, E., Southan, C., Pawson, A. J., Ireland, S., ... NC-IUPHAR. (2018). The IUPHAR/BPS Guide to PHARMACOLOGY in 2018: Updates and expansion to encompass the new guide to IMMUNOPHARMACOLOGY. *Nucleic Acids Research*, 46(D1), D1091–D1106. <https://doi.org/10.1093/nar/gkx1121>
- Huang, L., Wang, C. F., Serhan, C. N., & Strichartz, G. (2011). Enduring prevention and transient reduction of postoperative pain by intrathecal resolvin D1. *Pain*, 152(3), 557–565. <https://doi.org/10.1016/j.pain.2010.11.021>
- Jin, X., & Gereau, R. W. (2006). Acute p38-mediated modulation of tetrodotoxin-resistant sodium channels in mouse sensory neurons by tumor necrosis factor- α . *The Journal of Neuroscience*, 26(1), 246–255. <https://doi.org/10.1523/JNEUROSCI.3858-05.2006>
- Kawasaki, Y., Zhang, L., Cheng, J. K., & Ji, R. R. (2008). Cytokine mechanisms of central sensitization: Distinct and overlapping role of interleukin-1 β , interleukin-6, and tumor necrosis factor- α in regulating synaptic and neuronal activity in the superficial spinal cord. *The Journal*

- of *Neuroscience*, 28(20), 5189–5194. <https://doi.org/10.1523/JNEUROSCI.3338-07.2008>
- Kilkenny, C., Browne, W., Cuthill, I. C., Emerson, M., Altman, D. G., & Group NCRGW (2010). Animal research: Reporting in vivo experiments: The ARRIVE guidelines. *British Journal of Pharmacology*, 160(7), 1577–1579.
- Kolaczowska, E., & Kubes, P. (2013). Neutrophil recruitment and function in health and inflammation. *Nature Reviews. Immunology*, 13(3), 159–175. <https://doi.org/10.1038/nri3399>
- Levy, B. D., Clish, C. B., Schmidt, B., Gronert, K., & Serhan, C. N. (2001). Lipid mediator class switching during acute inflammation: signals in resolution. *Nature Immunology*, 2(7), 612–619. <https://doi.org/10.1038/89759>
- Liao, H. Y., Hsieh, C. L., Huang, C. P., & Lin, Y. W. (2017). Electroacupuncture attenuates CFA-induced inflammatory pain by suppressing Nav1.8 through S100B, TRPV1, opioid, and adenosine pathways in mice. *Scientific Reports*, 7, 42531.
- Ma, Q. P., & Woolf, C. J. (1996). Progressive tactile hypersensitivity: An inflammation-induced incremental increase in the excitability of the spinal cord. *Pain*, 67(1), 97–106. [https://doi.org/10.1016/0304-3959\(96\)03105-3](https://doi.org/10.1016/0304-3959(96)03105-3)
- Maruyama, K., Takayama, Y., Kondo, T., Ishibashi, K. I., Sahoo, B. R., Kanemaru, H., ... Akira, S. (2017). Nociceptors boost the resolution of fungal osteoinflammation via the TRP channel-CGRP-Jdp2 axis. *Cell Reports*, 19(13), 2730–2742. <https://doi.org/10.1016/j.celrep.2017.06.002>
- Mika, J., Wawrzczak-Bargiela, A., Osikowicz, M., Makuch, W., & Przewlocka, B. (2009). Attenuation of morphine tolerance by minocycline and pentoxifylline in naive and neuropathic mice. *Brain, Behavior, and Immunity*, 23(1), 75–84. <https://doi.org/10.1016/j.bbi.2008.07.005>
- Osikowicz, M., Skup, M., Mika, J., Makuch, W., Czarkowska-Bauch, J., & Przewlocka, B. (2009). Glial inhibitors influence the mRNA and protein levels of mGlu2/3, 5 and 7 receptors and potentiate the analgesic effects of their ligands in a mouse model of neuropathic pain. *Pain*, 147(1–3), 175–186. <https://doi.org/10.1016/j.pain.2009.09.002>
- Park, C. K. (2015). Maresin 1 inhibits TRPV1 in temporomandibular joint-related trigeminal nociceptive neurons and TMJ inflammation-induced synaptic plasticity in the trigeminal nucleus. *Mediators of Inflammation*, 2015, 275126.
- Park, C. K., Xu, Z. Z., Liu, T., Lu, N., Serhan, C. N., & Ji, R. R. (2011). Resolvin D2 is a potent endogenous inhibitor for transient receptor potential subtype V1/A1, inflammatory pain, and spinal cord synaptic plasticity in mice: Distinct roles of resolvin D1, D2, and E1. *The Journal of Neuroscience*, 31(50), 18433–18438. <https://doi.org/10.1523/JNEUROSCI.4192-11.2011>
- Pavao-de-Souza, G. F., Zarpelon, A. C., Tedeschi, G. C., Mizokami, S. S., Sanson, J. S., Cunha, T. M., ... Verri, W. A. Jr. (2012). Acetic acid- and phenyl-p-benzoquinone-induced overt pain-like behavior depends on spinal activation of MAP kinases, PI(3)K and microglia in mice. *Pharmacology, Biochemistry, and Behavior*, 101(3), 320–328. <https://doi.org/10.1016/j.pbb.2012.01.018>
- Pinho-Ribeiro, F. A., Baddal, B., Haarsma, R., O'Seaghda, M., Yang, N. J., Blake, K. J., ... Chiu, I. M. (2018). Blocking neuronal signaling to immune cells treats streptococcal invasive infection. *Cell*, 173(5), 1083–1097. <https://doi.org/10.1016/j.cell.2018.04.006>
- Pinho-Ribeiro, F. A., Verri, W. A. Jr., & Chiu, I. M. (2017). Nociceptor sensory neuron-immune interactions in pain and inflammation. *Trends in Immunology*, 38(1), 5–19. <https://doi.org/10.1016/j.it.2016.10.001>
- Recchiuti, A., & Serhan, C. N. (2012). Pro-resolving lipid mediators (SPMs) and their actions in regulating miRNA in novel resolution circuits in inflammation. *Frontiers in Immunology*, 3, 298.
- Roberson, D. P., Gudes, S., Sprague, J. M., Patoski, H. A., Robson, V. K., Blasf, F., ... Woolf, C. J. (2013). Activity-dependent silencing reveals functionally distinct itch-generating sensory neurons. *Nature Neuroscience*, 16(7), 910–918. <https://doi.org/10.1038/nn.3404>
- Ruiz-Miyazawa, K. W., Pinho-Ribeiro, F. A., Zarpelon, A. C., Staurengo-Ferrari, L., Silva, R. L., Alves-Filho, J. C., ... Verri, W. A. Jr. (2015). Vinpocetine reduces lipopolysaccharide-induced inflammatory pain and neutrophil recruitment in mice by targeting oxidative stress, cytokines and NF- κ B. *Chemico-Biological Interactions*, 237, 9–17. <https://doi.org/10.1016/j.cbi.2015.05.007>
- Scholz, J., & Woolf, C. J. (2007). The neuropathic pain triad: Neurons, immune cells and glia. *Nature Neuroscience*, 10(11), 1361–1368. <https://doi.org/10.1038/nn1992>
- Serhan, C. N. (2017). Treating inflammation and infection in the 21st century: New hints from decoding resolution mediators and mechanisms. *The FASEB Journal*, 31(4), 1273–1288. <https://doi.org/10.1096/fj.201601222R>
- Serhan, C. N., Chiang, N., Dalli, J., & Levy, B. D. (2015). Lipid mediators in the resolution of inflammation. *Cold Spring Harbor Perspectives in Biology*, 7(2), a016311. <https://doi.org/10.1101/cshperspect.a016311>
- Serhan, C. N., Dalli, J., Karamnov, S., Choi, A., Park, C. K., Xu, Z. Z., ... Petasis, N. A. (2012). Macrophage proresolving mediator maresin 1 stimulates tissue regeneration and controls pain. *The FASEB Journal*, 26(4), 1755–1765. <https://doi.org/10.1096/fj.11-201442>
- Sinatra, R. (2010). Causes and consequences of inadequate management of acute pain. *Pain Medicine*, 11(12), 1859–1871. <https://doi.org/10.1111/j.1526-4637.2010.00983.x>
- Talbot, S., Abdounour, R. E., Burkett, P. R., Lee, S., Cronin, S. J., Pascal, M. A., ... Woolf, C. J. (2015). Silencing nociceptor neurons reduces allergic airway inflammation. *Neuron*, 87(2), 341–354. <https://doi.org/10.1016/j.neuron.2015.06.007>
- Verri, W. A. Jr., Cunha, T. M., Parada, C. A., Poole, S., Cunha, F. Q., & Ferreira, S. H. (2006). Hypernociceptive role of cytokines and chemokines: Targets for analgesic drug development? *Pharmacology & Therapeutics*, 112(1), 116–138. <https://doi.org/10.1016/j.pharmthera.2006.04.001>
- Woolf, C. J. (1983). Evidence for a central component of post-injury pain hypersensitivity. *Nature*, 306(5944), 686–688. <https://doi.org/10.1038/306686a0>
- Woolf, C. J. (1994). A new strategy for the treatment of inflammatory pain. Prevention or elimination of central sensitization. *Drugs*, 47(Suppl 5), 1–9. discussion 46–47
- Xu, Z. Z., Zhang, L., Liu, T., Park, J. Y., Berta, T., Yang, R., ... Ji, R. R. (2010). Resolvins RvE1 and RvD1 attenuate inflammatory pain via central and peripheral actions. *Nature Medicine*, 16(5), 592–597. 591p following 597
- Yekkirala, A. S., Roberson, D. P., Bean, B. P., & Woolf, C. J. (2017). Breaking barriers to novel analgesic drug development. *Nature Reviews. Drug Discovery*, 16, 810. <https://doi.org/10.1038/nrd.2017.202>
- Yu, Y.-Q., Zhao, F., Guan, S.-M., & Chen, J. (2011). Antisense-mediated knockdown of Nav1.8, but not Nav1.9, generates inhibitory effects on complete Freund's adjuvant-induced inflammatory pain in rat. *PLoS One*, 6(5), e19865.
- Zarpelon, A. C., Rodrigues, F. C., Lopes, A. H., Souza, G. R., Carvalho, T. T., Pinto, L. G., ... Verri, W. A. Jr. (2016). Spinal cord oligodendrocyte-

- derived alarmin IL-33 mediates neuropathic pain. *The FASEB Journal*, 30(1), 54–65. <https://doi.org/10.1096/fj.14-267146>
- Zhang, J. L., Zhuo, X. J., Lin, J., Luo, L. C., Ying, W. Y., Xie, X., ... Jin, S. W. (2017). Maresin1 stimulates alveolar fluid clearance through the alveolar epithelial sodium channel Na, K-ATPase via the ALX/PI3K/Nedd4-2 pathway. *Laboratory Investigation*, 97(5), 543–554. <https://doi.org/10.1038/labinvest.2016.150>
- Zhang, L., Terrando, N., Xu, Z. Z., Bang, S., Jordt, S. E., Maixner, W., ... Ji, R. R. (2018). Distinct analgesic actions of DHA and DHA-derived specialized pro-resolving mediators on post-operative pain after bone fracture in mice. *Frontiers in Pharmacology*, 9, 412. <https://doi.org/10.3389/fphar.2018.00412>
- Zhu, M. D., Zhao, L. X., Wang, X. T., Gao, Y. J., & Zhang, Z. J. (2014). Ligustilide inhibits microglia-mediated proinflammatory cytokines production and inflammatory pain. *Brain Research Bulletin*, 109, 54–60. <https://doi.org/10.1016/j.brainresbull.2014.10.002>

How to cite this article: Fattori V, Pinho-Ribeiro FA, Staurengo-Ferrari L, et al. The specialised pro-resolving lipid mediator maresin 1 reduces inflammatory pain with a long-lasting analgesic effect. *Br J Pharmacol.* 2019;176: 1728–1744. <https://doi.org/10.1111/bph.14647>